

## Extension of a DNA Molecule by Local Heating with a Laser

Masatoshi Ichikawa,<sup>1</sup> Hiroki Ichikawa,<sup>2</sup> Kenichi Yoshikawa,<sup>3</sup> and Yasuyuki Kimura<sup>1</sup>

<sup>1</sup>*Department of Physics, Graduate School of Sciences, Kyushu University, Fukuoka 812-8581, Japan*

<sup>2</sup>*Earthquake Research Institute, The University of Tokyo, Tokyo 113-0032, Japan*

<sup>3</sup>*Department of Physics, Graduate School of Science, Kyoto University, Kyoto 606-8502, Japan*

(Received 16 November 2006; published 5 October 2007)

Thermal convection and thermophoresis induced by  $\mu\text{m}$ -scale local heating are shown to elongate a single DNA molecule. An infrared laser used as a point heat source is converged into a dispersion solution of DNA molecules, which is observed under a fluorescent microscope. The thermal convection around the laser focus manifests as extensional flow for the long DNA chain. A simulation of thermal convection that reproduces the experimental condition provides numerical support for the stretching caused by thermal convection. This DNA elongation technique is a novel method for manipulating the intact single DNA molecules, and it can be applied to a “lab on a chip”.

DOI: [10.1103/PhysRevLett.99.148104](https://doi.org/10.1103/PhysRevLett.99.148104)

PACS numbers: 87.14.Gg, 47.55.pb, 87.83.+a

Over the past two decades, developments in molecular biology and micro- or nanotechnology have increased the interest of scientists and engineers in the mechanical manipulation of single biomacromolecules. In particular, by using various manipulation techniques, investigations of DNA have contributed to developments in polymer physics, biophysics, and genome analysis [1].

A long DNA molecule, e.g., longer than  $50\ \mu\text{m}$ , assumes several  $\mu\text{m}$ -sized random coil conformations in solution due to entropic elasticity. Thus, to elongate a DNA molecule, an external force must be applied. The relationship between such an external force and the deformation of a polymer chain has been theoretically established, and the relevant theories have successfully explained polymer-stretching dynamics such as the direction of birefringence within a fluidic molten polymer [2]. With a fluorescently labeled DNA molecule, it is also possible to visualize the change in the conformation of a single polymer under an optical microscope. For example, a DNA molecule that has a total length of several dozen micrometers is forced and elongated in response to hydrodynamic flow [3]. Such DNA-stretching experiments have been demonstrated at the center of two opposite fluxes in a cross-slot geometry, which is often referred to as elongational flow [4]. Moreover, other DNA-stretching experiments have also been reported, e.g., simple unidirectional flow [5], shear flow in an evaporating droplet [6], electroosmotic flow under dc voltage [7], and elongational flow using dielectric interaction [8]. It has been shown that a strong electric field alone extends DNA molecules, e.g., an alternating voltage applied to a long DNA chain dispersed in a polymer solution or in gel [9,10], a high-frequency ac field or dielectrophoresis in water [11], etc. On the other hand, straightforward methods have also been investigated; e.g., a DNA chain adhered to microbeads at one or both ends is mechanically stretched by manipulation of the microbeads using micropipettes and/or optical tweezers

[1,12–14]. The latter method has been actively used to measure forces in biophysical experiments related to DNA molecules.

In this Letter we will describe a novel phenomenon pertaining to the elongation of a long DNA molecule under focused infrared laser light irradiation without any modification of the molecule. Stretching of the DNA molecule is attributed to combination of thermal convection and thermophoresis caused by microheating due to the convergent laser.

We used a double-stranded DNA (T4GT7 DNA, 166 kbp, Nippon Gene) with a full length of ca.  $56\ \mu\text{m}$  stained with YOYO-1 (Molecular Probes). The materials had been premixed in Milli-*Q* water or in heavy water (EURISO-TOP) in final concentrations of  $0.1\ \mu\text{M}$  for the base-pair concentration of DNA,  $0.01\ \mu\text{M}$  YOYO-1, 4%(v/v) mercaptoethanol, and 100 mg/mL dextran (av. MW =  $7.5 \times 10^4$ , Sigma). The sample solution was enclosed in a glass cell that gave a solution thickness of approximately  $50\ \mu\text{m}$ . The laser irradiation and microscopic observations were performed using a large-aperture oil-immersion objective lens ( $\times 100$  UPlanApo for ir, NA = 1.35) on a fluorescent microscope (IX-70, Olympus). An infrared Nd:YAG laser (CW 1064 nm, random polarization, TEM<sub>00</sub>) for local heating was converged to a point approximately  $1\ \mu\text{m}$  in diameter in the observation field through the objective lens. The incident laser beam power measured before the objective lens was approximately 2 W. It has been shown that a focused laser can trap a DNA molecule by using moderate laser power ( $\leq 1$  W) in a polyethylene glycol solution [15]. Fluorescent images of single DNA molecules were captured by an EB-CCD video camera (C7190-43, HAMAMATSU Photonics).

The parameters adopted in the hydrodynamic simulations were as follows. Kinematic viscosity:  $\nu = 3 \times 10^{-6}$  to  $\nu = 1 \times 10^{-6}\ \text{m}^2/\text{s}$  (fitting the temperature dependence

of experimental measurements by a rotary viscometer), coefficient of volume expansion:  $\alpha = 2.1 \times 10^{-4} \text{ K}^{-1}$  (value of pure water), thermal diffusivity:  $\kappa = 0.133 \times 10^{-6} \text{ m}^2/\text{s}$  (experimental measurement), density:  $\rho_0 = 1.038 \text{ g/cm}^3$  (ditto), ratio of specific heat:  $c_p = 0.959$  (ditto). The boundary condition was set by a cylindrical symmetric system, where the vertical  $z$  axis along the laser light line was  $50 \mu\text{m}$  high, the horizontal radial axis  $r$  was  $200 \mu\text{m}$  in radius, the numerical resolution of the fluid was  $200 \times 800$ , and the volume factor was weighted with  $2\pi r$  to construct the cylindrical system  $(r, \theta, z)$  for two-dimensional calculations. Laser heating was calculated by assuming self-heat generation for each numerical cell to make it proportional to the light power in the respective cells. We assumed that the 1064 nm laser light was absorbed in the solution with an absorption coefficient of  $0.15 \text{ cm}^{-1}$ ; the corresponding heat generation is  $1.5 \times 10^{-5} \text{ W}$  per  $1 \mu\text{m}$  slice and per 1 W light power. The above absorbance is calculated from the absorption coefficient of pure water for light with a wavelength of 1064 nm [16]. The power of the laser was  $P_0 = 2 \text{ W}$ . The laser light profile was approximated to be Gaussian and Lorentzian with convergence expressed by  $P(r, z) = P_0 \frac{2}{\pi(z^2 + \omega_0^2)} \times \exp\left(\frac{-2r^2}{z^2 + \omega_0^2}\right)$ , where the beam waist was given as  $\omega_0 = 0.5 \mu\text{m}$ . The rate of heat generation  $H(r, z) \propto P(r, z)$  was obtained by integrating the contributions of subcells—1/100 of the cell. Walls with a no-slip condition at the top and bottom, and at  $r = 200 \mu\text{m}$  were configured and fixed for the heat bath at  $T_0 = 20^\circ\text{C}$  to simulate deviation from room temperature. Gravity was considered to pull downward, i.e., along  $-z$ . The calculations were performed using the finite volume method with the Boussinesq approximation given below:

$$\nabla \cdot \mathbf{u} = 0, \quad (1)$$

$$\frac{D\mathbf{u}}{Dt} = -\frac{1}{\rho_0} \nabla p + \frac{1}{\rho_0} \nabla \cdot \boldsymbol{\tau} - g[1 + \alpha(T_0 - T)]\mathbf{e}_z, \quad (2)$$

$$\frac{DT}{Dt} = \kappa \nabla^2 T + \frac{H(r, z)}{c_p \rho_0}, \quad (3)$$

where  $\mathbf{u}$ ,  $\boldsymbol{\tau}$ ,  $p$ , and  $g$  are the flow velocity vector, the deviatoric stress tensor, pressure, and gravitational acceleration, respectively.

Figure 1 shows a typical result. The white bodies in the pictures indicate the fluorescence from a DNA molecule. The internal and translational Brownian motions of the DNA chain are represented by the fluctuation and diffusion of the fluorescent signal. Long-range fluctuation along the DNA chain is appreciably reduced in viscous dextran solution compared to water or a buffer solution. When the infrared laser is introduced into a spot on the observation focal plane, the DNA molecule(s) starts stretching, as shown in Fig. 1, and reaches a long-axis diameter of approximately  $20\text{--}25 \mu\text{m}$  after 30 s of irradiation

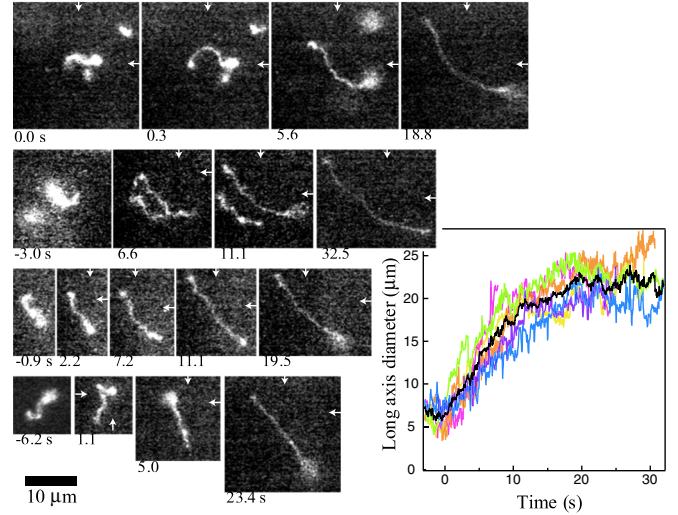


FIG. 1 (color online). A single DNA molecule under laser irradiation. The intersection points of the white arrows in each panel indicate the laser focus. The free DNAs in the dextran solution just before laser illumination are displayed at the left end with negative time values. The horizontal time axis on the right-hand graph corresponds to the time specified under each picture. The graph shows the time development of the long-axis length for six independent DNA-stretching observations and the average line (black).

(Fig. 1). This is approximately 5 times longer than the initial value and is 35% to 45% of the full length. The movie provided in the supplemental material shows efficient elongation of the DNA segment near the focus [17]. In the movie, the DNAs located near the upper glass plate of the chamber slowly move upwards without contacting and adhering to the plate. In addition to the targeted DNA molecule, neighboring DNA molecules also tend to be elongated.

Such elongation is generated in a reproducible manner when the focus is located in the solution near the surface of the upper glass plate. However, the effect disappears when the focus is situated in the middle or bottom region of the solution. The DNAs are driven upward by the convective motion of the solution.

Next, we performed the same experiment with a  $\text{D}_2\text{O}$  solvent to clarify the effect of laser heating. The solution contained over 95% (v/v)  $\text{D}_2\text{O}$  and showed an absorption of 1/10 or lower for a 1064 nm light relative to that for a  $\text{H}_2\text{O}$  solvent [18]. Figure 2 shows the change in the conformation of DNA with laser irradiation in  $\text{H}_2\text{O}$  (open circle) and  $\text{D}_2\text{O}$  (closed circle). In this figure, laser irradiation is performed near the top end. The graph indicates that DNA elongation does not occur with the  $\text{D}_2\text{O}$  solvent or in the low-heating condition.

The above experimental results suggest that DNA stretching is due to the thermal effect of local heating by the laser. Other possibilities, such as electromagnetic effects of the laser light, can be excluded. We can consider as distinct cases polymer clustering or phase separation gen-

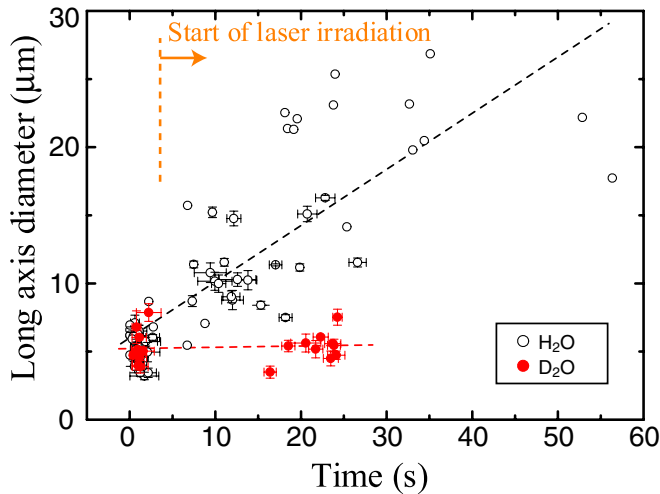


FIG. 2 (color online). Experimental results of DNA elongation for light water and heavy water. The initial long-axis diameters of the DNAs in each solution for time values around zero are plotted in the lower left, and the diameters after laser irradiation are plotted on the right. The broken lines are linear regression fitting lines for each condition.

erated by the dielectric effect of focused light or laser trapping which depletes the DNA from the focus [18]. However, since we did not observe a phase boundary or cluster with phase contrast microscopy, such cases can also be excluded. Thus, we conclude that thermal convection and/or thermophoresis causes DNA elongation. Among thermal convection and thermophoresis [19], thermophoresis, often called the Ludwig-Soret effect, by itself cannot explain the experimental results, in that DNA molecules at the bottom or intermediate heights in the solution were not stretched. Consequently, we quantitatively estimate the contribution of thermal convection induced by laser heating in the elongation of DNA chains.

Since the present experimental setup has axial symmetry with respect to the geometry of the optical cone, it is expected that the extensional flow near the top of the solution would form a source-like streamline around the focus. An ideal two-dimensional source shows dependence given by  $v_r \propto 1/r$ , where  $v_r$  and  $r$  are the  $r$  elements of the flow velocity and radial distance, respectively. However, it seems unrealistic to claim that a  $\mu\text{m}$ -sized 2D source manifests itself in the real experimental system, considering the system size, viscosity, size of the heating area, etc. Therefore, we performed a thermal convection simulation that reproduced the experimental conditions to clarify the current profile around the laser focus.

Figure 3 shows the simulation results corresponding to heating of the top end:  $z = 40 \mu\text{m}$ . The panel denotes the stationary state, where the state is adequately stable because this fluidic system is estimated to have laminar flow (Reynolds number  $\ll 1$ ). The thermal distributions almost reach a steady level on a time scale on the order of  $1/100$  s. The result shows divergent flow near the upper side plate as  $v_r \propto r$ , similar to the previous elongational flow [3].

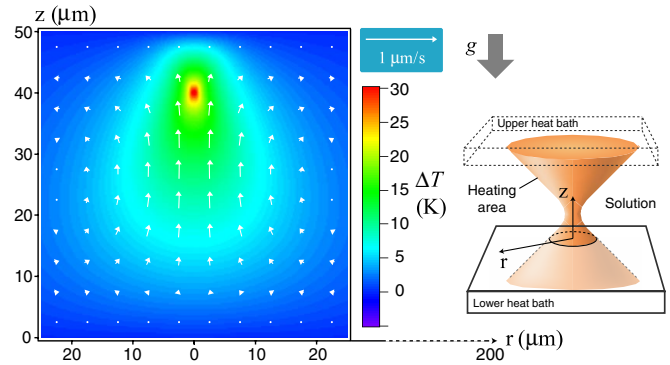


FIG. 3 (color online). Results of the thermal convection simulation. The temperature difference of the cell correlates with the color index bar, and current vectors are denoted as arrows in the images. The heating spot is located at  $(r, z) = (0, 40) \mu\text{m}$ .

To compare the experiments, we consider the vicinity of the flux around the heat spots because the present experimental system limits the observable area to a few micrometers in thickness and to the height of the laser heating focus. The top-end region indicates an  $r$ -directional spreading current with slower  $z$ -directional pushing around the heating focus. The profiles of the flow velocity and  $\partial v_r / \partial r$ ,  $\partial v_r / \partial z$  are described in Fig. 4.

The heavy-water condition is also predictable by the results. Since almost all of the generated heat in the present simulation system dissipates immediately into the heat bath through diffusion, and since the solutions do not show turbulent flow, the flow speed and temperature differences  $\Delta T$  can be approximately assumed to be linearly proportional to the heat generation or absorbed energy of the laser beam. The heavy-water experiment would exhibit 1/10 or lower absorption at a wavelength of 1064 nm compared to the light-water condition. Thus, the flow speed for the heavy-water condition would also exhibit changes amounting to 1/10 or less.

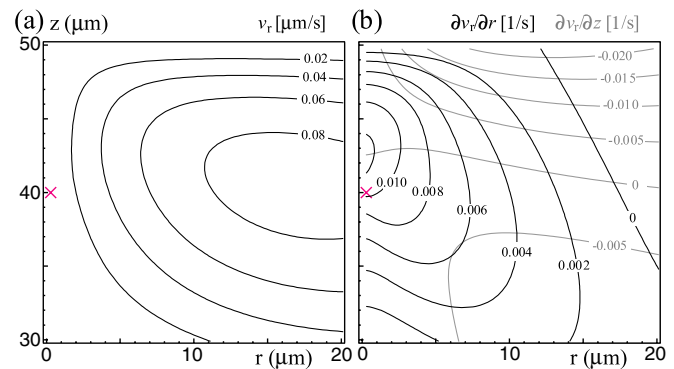


FIG. 4 (color online). Distributions of flow velocity and strain/shear rates in the simulation result. The focus of the heating is at  $(r, z) = (0, 40) \mu\text{m}$ , and the plotted profiles consider the  $r$  direction elements around the heat spot. (a) The contour lines of flow velocity profile  $v_r$ . (b) The contour line image denotes the distribution of the extensional strain  $\partial v_r / \partial r$  and shear strain  $\partial v_r / \partial z$  around the focus.

We will now discuss the degree of DNA elongation as inferred from the strain rate based on data from previous theoretical and experimental studies. The flow profile can be assumed to obey the relation  $v_r \propto r$  around the laser focus. DNA elongation in this type of flow profile has been well studied in past experiments on elongational flow where it was constructed from two opposite currents using a cross-channel microfluidic device [3]. Meanwhile, the flow vector in our experiment describes a radial pattern near the plate. The hydrodynamic stress applied to the DNA is mainly composed of four terms [17],  $\partial v_r/\partial r$ : extensional strain for  $r$  direction (dominant strain rate in Ref. [3]),  $\partial v_r/\partial z$ : shear rate along a perpendicular element,  $v_r/r$ : extensional strain for  $\theta$  direction (spreading or converging), and  $\partial v_z/\partial z$ : that in the  $z$  component. First, DNA stretching by the strain rate  $s$  (1/s) has been well established by cross-channel experiments as a simple relation between  $s$  and the longest relaxation time of the long-axis diameter length of the extended DNA  $t_{\text{relax}}$ . This study showed that  $s \sim 0.04$  (1/s) is required [3] to suffuse the present typical result: the DNA-stretching ratio for the contour length: 0.4 and  $t_{\text{relax}} = 28$  s. On the other hand, the present extensional strain along the current is estimated to be  $s \sim 0.010$  (1/s) around the heating focus. The order of magnitude of  $\partial v_r/\partial r$  in the simulation agrees with the experimental trend; however, the value is rather small to stretch the DNA sufficiently. Furthermore, the shear stress  $\partial v_r/\partial z$  in the present experiment is caused by the no-slip condition on the glass plate. The shear  $\partial v_r/\partial z$  has been compared with the  $\partial v_r/\partial r$  extensional strain rate in Ref. [13] as 0.2 to 0.4 times the efficiency for stretching DNA. In the present case in which the DNA molecule lies across the stagnation point, the stresses at the ends of the DNA have opposite directions; thus, the tumbling element of the shear stresses applied to the respective edges of the DNA may counteract each other at the center of the DNA. This tumbling has been reported to reduce the efficiency of stretching [13]. The order of magnitude of the shear stress itself is equal to or greater than the strain rate along the current. The third current gradient,  $v_r/r \approx 0.012$  around the focus, shows a force direction that differs from those of the above two stresses. Although the radial stress becomes almost negligible when the DNA is just across the stagnation point, this radially spreading stress should extend the DNA effectively like a circular arc when the stagnation point is crossed. Stretching of the arc is often observed in experiments, such as in Fig. 1. The last  $\partial v_z/\partial z$ , which indicates a reduction in the speed of the flow around the focus, does not contribute to DNA stretching in the  $r\theta$  plane.

Each strain estimated from the simulation is less than those in previous studies. While the strains can additively affect DNA stretching, the distributions of the strains are not exactly the same. Some factors that may alleviate this shortage can be suggested, but without clear evidence. The present study used a dextran solution to lengthen the relaxation time of DNA; however, the relaxation time in

a polymer solution is not the same as that in a Newtonian solution, even at the same viscosity [20]. In addition, light pressure can enhance the convective motion of the solution. When we apply a laser power of 3 W or higher,  $\mu\text{m}$ -sized roll convections manifest around the focus. The simulation excludes such unidirectional light pressure and rheological properties of the polymer solution, which may contribute to the acceleration of convective motion and generate slight roll. Very recently, it has been reported that thermophoresis generated by a focused laser can repel a single DNA molecule under a convection-suppressed condition in a solution with a certain ionic strength [19]. Both thermophoresis and thermal convection may stretch DNA under the present top setting of the heating focus, and the bottom settings may make them cancel each other out for stretching.

The present easy-handling technique, e.g., local convection at a desired position, could be useful for the manipulation and analysis of a single DNA molecule by using fluorescent *in situ* hybridization (FISH) techniques in a lab-on-a-chip or plate system. However, in such applications, a laser light at a higher absorption wavelength or a heating microfilament should be used for more efficient stretching.

We are thankful to Dr. H. Oana and Dr. M. Takenaka for their support with the experiments.

- 
- [1] C. Bustamante *et al.*, Nature (London) **421**, 423 (2003).
  - [2] P. G. De Gennes, J. Chem. Phys. **60**, 5030 (1974).
  - [3] T. T. Perkins *et al.*, Science **276**, 2016 (1997).
  - [4] E. S. G. Shaqfeh, J. Non-Newtonian Fluid Mech. **130**, 1 (2005).
  - [5] S. B. Smith *et al.*, Science **258**, 1122 (1992).
  - [6] A. Bensimon *et al.*, Science **265**, 2096 (1994).
  - [7] O. B. Bakajin *et al.*, Phys. Rev. Lett. **80**, 2737 (1998).
  - [8] M. Nakano *et al.*, Appl. Phys. Lett. **89**, 133901 (2006).
  - [9] M. Ueda *et al.*, Polymer Journal **29**, 1040 (1997).
  - [10] N. Kaji *et al.*, Biophys. J. **82**, 335 (2002).
  - [11] M. Washizu *et al.*, IEEE Trans. Ind. Appl. **26**, 1165 (1990).
  - [12] T. T. Perkins *et al.*, Science **264**, 819 (1994).
  - [13] D. E. Smith *et al.*, Science **283**, 1724 (1999).
  - [14] C. Hoyer *et al.*, J. Biotechnol. **52**, 65 (1996).
  - [15] M. Ichikawa *et al.*, J. Phys. Soc. Jpn. **74**, 1958 (2005).
  - [16] K. Svoboda and S. M. Block, Annu. Rev. Biophys. Biomol. Struct. **23**, 247 (1994).
  - [17] See EPAPS Document No. E-PRLTAO-99-055739 for a movie that shows the stretching of single DNA molecules. For more information on EPAPS, see <http://www.aip.org/pubservs/epaps.html>.
  - [18] M. Ishikawa *et al.*, Bull. Chem. Soc. Jpn. **69**, 59 (1996).
  - [19] D. Braun and A. Libchaber, Phys. Rev. Lett. **89**, 188103 (2002); S. Duhr and D. Braun, Proc. Natl. Acad. Sci. U.S.A. **103**, 19678 (2006).
  - [20] The measured relaxation time is longer than the previous experimental result [13]. This may be because the ambient polymer confines a DNA chain to reptative motion.